Available online at www.sciencedirect.com
ScienceDirect
Optics Communications 281 (2008) 3776–3780
OPTICS COMMUNICATIONS
www.elsevier.com/locate/optcom

Highly efficient THz emission from differently grown InN at 800 nm and 1060 nm excitation

G. Matthäus [a,*], V. Cimalla [b], B. Pradarutti [c], S. Riehemann [c], G. Notni [c], V. Lebedev [b], O. Ambacher [b], S. Nolte [a], A. Tünnermann [a,c]

[a] Friedrich Schiller University Jena, Institute of Applied Physics, Max-Wien-Platz 1, Jena D-07743, Germany
[b] Technical University Ilmenau, Institute of Micro- and Nanotechnology, Kirchhofstrasse 7, Ilmenau D-98693, Germany
[c] Fraunhofer Institute for Applied Optics and Precision Engineering, Albert-Einstein-Strasse 7, Jena, D-07745, Germany

Received 19 November 2007; accepted 16 March 2008

Abstract

A detailed study on differently molecular-beam epitaxy (MBE) grown InN wavers as THz surface emitters is reported. The samples were excited using 120 fs and 100 fs short laser pulses delivered by a Ti:Sapphire oscillator at 800 nm and a fiber laser amplifier at 1060 nm, respectively. The InN emission properties are compared to a p-type InAs reference sample. At 800 nm, atomically smooth InN with low background electron concentration exhibits slightly stronger THz emission than the well-established p-InAs emitter. This high THz efficiency of InN is reported for the first time. The strong emission of InN is caused by the absence of any intervalley scattering, which in the case of InAs, increases the effective mass of the photogenerated electrons and, thus, reduces the photo-Dember effect, which is most responsible for THz emission. Consequently, InN is a reliable material for strong THz emission.

Keywords: Terahertz; Surface emitter; InN; Ultrafast lasers

1. Introduction

The terahertz (THz) region of the electromagnetic spectrum (10^{11}–10^{13} Hz) has potential applications in many fields of science and technology, extending from spectroscopy, medical imaging, nondestructive materials testing through homeland security [1–5]. It was found by Zhang et al. [6] in 1990 that ultrashort THz pulses can be generated by illuminating semiconductor surfaces with femtosecond laser pulses. Typically InAs is used as the emitter material, however, also the emission of THz radiation from InN using a common Ti:Sapphire laser has been demonstrated [7]. The potential of these narrow band gap semiconductors (note that the band gap for InN has been revised from 1.9–2 eV to less than 0.8 eV, recently [8]) is the use of powerful fiber laser systems working at longer wavelengths, in particular at 1060 nm [9] or 1550 nm (the telecommunication regime) [10]. In contrast to conventional Ti:Sapphire systems, fiber lasers offer higher average power and can be designed as most compact systems [11].

InN provides a very strong absorption coefficient ($\approx 10^4\ cm^{-1}$, [12]), a high saturation velocity ($>1.5 \times 10^7$ cm/s, [13]) and has an extraordinary energy band structure yielding high electron mobilities ($\mu_n \approx 3500$ cm/Vs, [14]) over a wide range of excitation wavelengths. Hence, a more efficient InN-based THz source compared to the commonly established arsenides like GaAs or InAs could be expected.

Here, we present a detailed investigation of differently MBE grown InN layers as THz surface emitters excited at 800 and 1060 nm. We compare the InN measurements to a p-doped InAs emitter, which is known as the strongest surface emitter [15]. All InN layers show significant THz

* Corresponding author. Tel.: +49 3641 947824; fax: +49 3641 947802.
E-mail address: matthaeus@iap.uni-jena.de (G. Matthäus).
URL: http://www.iap.uni-jena.de (G. Matthäus).

0030-4018/$ - see front matter © 2008 Elsevier B.V. All rights reserved.
doi:10.1016/j.optcom.2008.03.057

emission. One sample even slightly exceeds the emission of our InAs reference sample.

The discussion of the origin of the strong surface emission is based on an ultrafast charge transport phenomena in an intrinsic surface field or due to the photo-Dember effect. However, these two models can not sufficiently explain the peculiar high THz emission from InN.

In this paper, we present a detailed study of the dependence of THz emission on the InN film properties. Moreover, we provide an extension of the theoretical models by taking into account the peculiarities of the InN band structure. It considers the low band gap, the high electron mobility and the reduced probability of intervalley scattering.

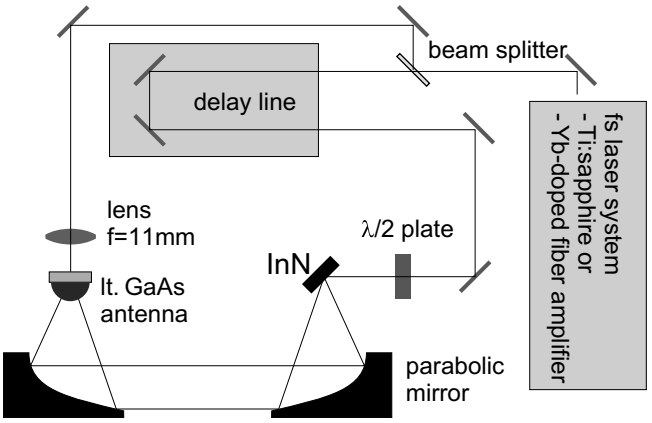

Fig. 1. Schematic for the THz-TDS.

2. Experiment

The InN layers were grown by plasma-induced MBE on various epitaxial templates as described in [16]. The thickness of the InN layers have been varied from 0.35 to 2.20 μm. The according layer properties are summarized in Table 1.

For the detection of the InN surface emission we used a common THz time domain system (TDS, see Fig. 1). More details on the setup can be found in [9].

For pumping the InN samples at 800 nm we used a Ti:Sapphire oscillator, delivering 120 fs short pulses at a repetition rate of 75 MHz. The maximum average output power was about 1.2 W. The pump source at 1060 nm, a self developed parabolic fiber amplifier system [17], delivered 100 fs pulses at the same repetition rate with a maximum average output power of about 12 W. In the experiment only 1.5 W were used in order to have similar experimental conditions compared to the Ti:Sapphire system. The excitation was performed at an angle of 45° with a laser spot size of approximately 2 mm at the semiconductor surface. The polarization was parallel to the plane of incidence for best pump absorption. As a detector we used a photoconductive antenna on low-temperature grown GaAs. To overcome the band gap of GaAs (≈1.4 eV) during 1060 nm excitation we frequency doubled the gate beam via second harmonic generation (SHG) using a BBO crystal.

3. Results

Fig. 2 and 3 show the measured THz signal of three InN samples excited at 800 and 1060 nm, respectively. All THz amplitudes were normalized to the emission of p-doped InAs, measured under identical experimental conditions. The highest THz efficiency was obtained from sample 207 (see Table 1). At 800 nm excitation it even revealed a slightly higher THz emission than p-InAs. Such a high THz emission of InN is observed for the first time. Until now, the highest investigated THz emission of InN was only reported to be about the same order of magnitude or less compared to InAs [7,10].

However, the InN samples also show multiple negative echoes with a delay of about 7 ps (Figs. 2a and 3a). Zhang

Table 1
InN layer properties

Structure	No.	Th. (nm)	μ_n (cm^2/Vs)	n (cm^{-3})	Morphology (nm)	rms	FWHM (XRD)	THz amplitude for 800 nm excitation (%)	THz amplitude for 1060 nm excitation (%)
InN/AlN/SiC,Si	199	195	473	5.1×10^{18}	Columns	43	0.835°	31	64
InN/GaN/AlN/SiC,Si	204	760	1150	1.6×10^{18}	Columns	13	0.356°	10	12
InN/GaN/Sapphire	186	170	221	5.1×10^{18}	Columns	34	–	3	19
	188	450	503	5.1×10^{18}	Columns	15	0.355°	11	44
	189	650	671	5.1×10^{18}	columns	12	0.273°	9	28
InN/GaN/AlN/SiC,Si	205	796	910	1.3×10^{18}	3D	34	0.317°	19	60
InN/AlN/Sapphire	202	120	91	2.2×10^{20}	Pits	8	0.835°	4	11
	203	170	212	2.2×10^{19}	Deep pits	2.3	1.379°	9	8
	206	2000	1240	9.5×10^{17}	Pits	8	0.461°	23	36
InN/GaN/AlN/Sapphire	207	700	1300	1.6×10^{18}	2D, Small pits	2.3	0.446°	108	75

Layerthickness Th., electron mobility μ_n, electron concentration n, surface roughness (rms), full width at half maximum value (FWHM) of the (0002) InN reflection in X-ray-diffraction (XRD), THz peak amplitude excited at 800 nm and 1060 nm (normalized to InAs peak).

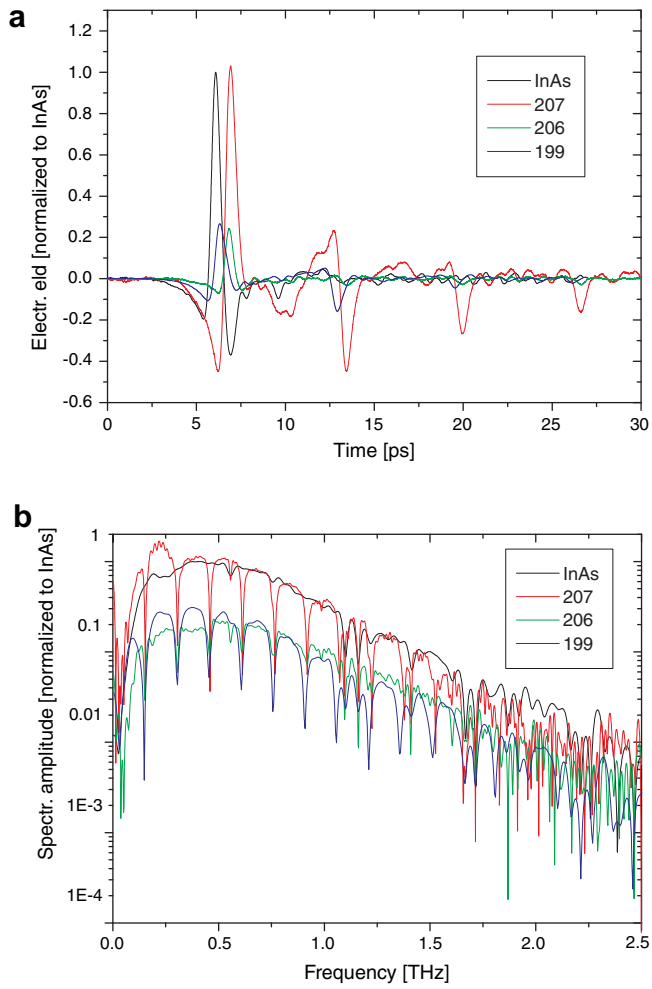

Fig. 2. Examples of InN emission during 800 nm excitation: (a) electric field amplitude, and (b) spectral amplitude.

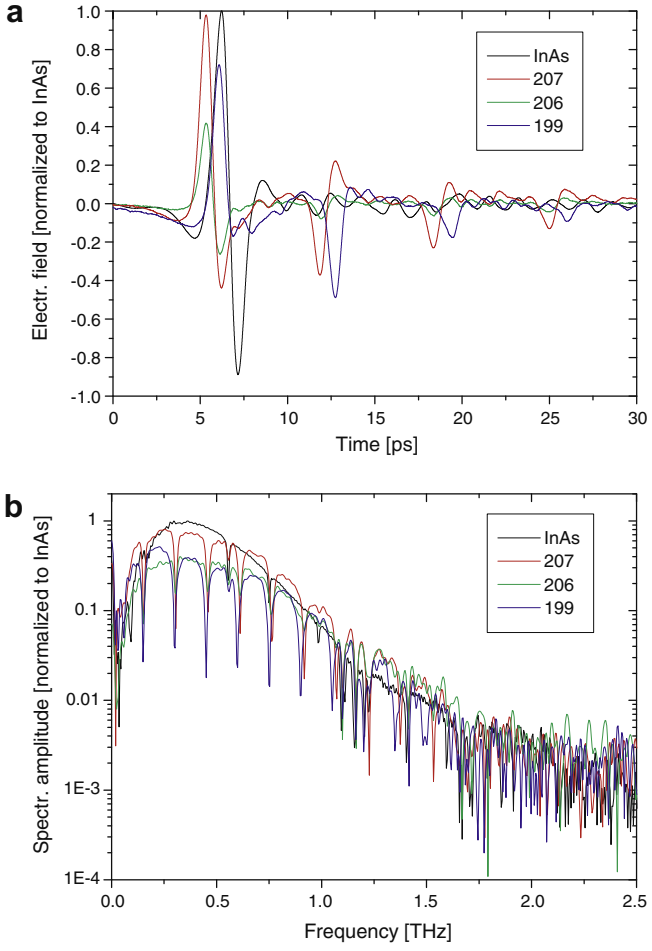

Fig. 3. Examples of InN emission during 1060 nm excitation: (a) electric field amplitude, and (b) spectral amplitude.

et al. have shown that THz generation due to the formation of a temporal electric dipole at semiconducting surfaces always yields an outward and an inward emitted THz wave and both waves have opposite signs [6]. Thus, the observed echo can be attributed to inner reflections of the inward emitted wave occurring at the sample's back and front facet. The substrate layers Al_2O_3 and SiC/Si basically amount the sample thicknesses of about 360 μm and are widely transparent for the THz regime. The buffer layers and the InN layer itself, contribute only a fraction of 0.1–2 μm. The according refractive indices are: $n_{AlN} \approx 3$, $n_{GaN} \approx 3$, $n_{Al_2O_3} \approx 3.2$ and $n_{SiC,Si} \approx 3.4$ [23,24]. Taking into account Snell's law and the substrate thicknesses, we estimate 6.5–7.5 ps delay, depending on the refractive indices. This is in good agreement with the experimental results.

The detected THz bandwidths of the InN layers were almost identical. They extend from about 0.1 GHz–2.5 THz and the maximum is located around 0.5 THz. However, one has to take into account the limited spectral response of the low-temperature grown GaAs antenna. The slightly narrower bandwidth at 1060 nm excitation results from gate pulse broadening during the SHG process, mentioned above. Recently, Chern et al. have also shown that the spectral width is almost independent of the excitation wavelength within a spectral range of 800–1550 nm [10]. The peak amplitudes of the investigated THz pulses were linearly increasing with the pump power, as expected for THz generation based on an optically excited transient photocurrent generation mechanism in the applied optical fluence regime [7,25].

Generally, the measurements show (see Table 1) an increased emission when the layer properties are improved, i.e. the electron concentration is decreased, the mobility is increased and the crystal is improved (FWHM in X-ray-diffraction) [7].

4. Discussion

The THz emission from semiconducting surfaces requires the formation of electric dipoles, which can be created by different mechanisms. First, an intrinsic electric field can separate the generated photo carriers and accelerate them in different directions. Such fields appear on the semiconductor surface in connection with depletion or enhancement zones. It has been observed that the polarity

of the THz emission of n-GaAs, n-InAs and p-InAs has the same direction [26], and our experiments revealed that InN behaves like InAs. However, the surface field of n-GaAs has an opposite orientation compared to n-InAs, p-InAs and InN, as schematically shown for n-GaAs and InN in Fig. 4. Thus, the surface field determines the THz emission only in the case of the depletion zones on wide band gap semiconductor surfaces (Fig. 4, GaAs). In the case of the accumulation zone of InN, the carrier density is very high and consequently, the width of the space charge region is only a few nm [27]. Thus, it has no dominant influence and can be neglected. Accordingly, the THz emission from InN has another origin, the photo-Dember effect [28]. The photo-Dember field occurs as a result of different diffusion coefficients of electrons and holes. The generated Dember field strength E_D reads [29]:

$$E_D \sim \frac{b\frac{d\Delta n}{dz}}{p_b + n_b b + \Delta n(1+b)} \quad \text{with } b = \frac{\mu_n}{\mu_p},$$

where μ_n and μ_p are the mobilities, n_b and p_b are the background concentration of electrons and holes, respectively, and Δn is the photo generated excess carrier density. This effect is particularly pronounced in narrow band gap semiconductors since these materials are characterized by high ratios b (see Table 2) and short optical absorption lengths due to the high absorption coefficient (see Fig. 5), causing a high gradient $d\Delta n/dz$ close to the surface. Thus, the THz emitting dipoles are created near the surface as well, which explains the superior emission properties of the smoothest InN sample. Table 2 and Fig. 5 show that InAs and InSb have high ratios b and at both excitation wavelengths (800 and 1060 nm) higher absorption coefficients than InN and should be consequently more efficient THz surface emitters in contrast to the experiments.

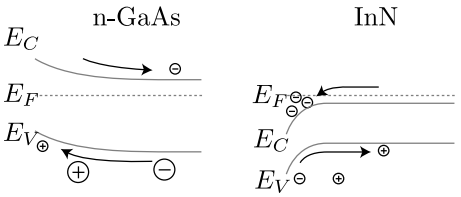

Fig. 4. Photo carrier separation in n-GaAs and InN due to surface band bending.

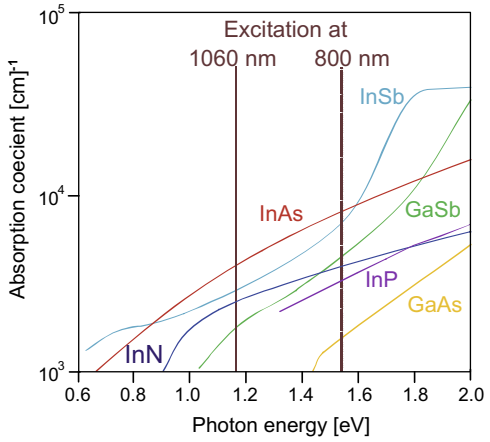

Fig. 5. Absorption coefficient for the semiconductors listed in Table 2; [30].

However, in low band gap materials the charge carriers exhibit a large kinetic energy after photo excitation yielding a pronounced intervalley scattering (see Fig. 6). For the cubic III–V semiconductors, the carriers in the L or X valleys have higher effective masses, which reduces the mobility. If the excitation energy is sufficiently high to populate these satellite valleys, the quotient b will be decreased and the Dember field is reduced as well. Table 2 lists the energy difference ΔE between the conduction band minima at the

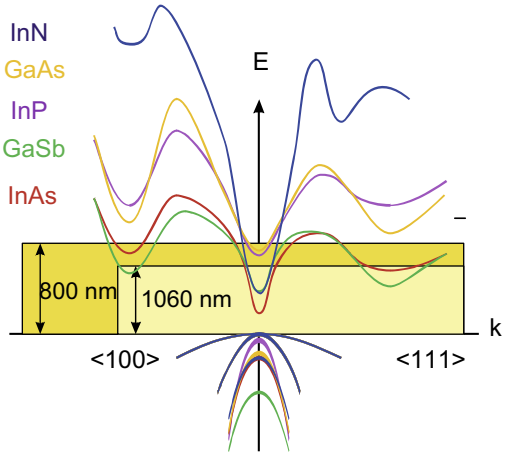

Fig. 6. Schematic of the energy bands for different THz emitting semiconductors in comparison to InN.

Table 2
Relevant material properties [18] and measured THz-emission efficiency at 800 nm [19]

Material	E_g (eV)	ΔE (eV)	μ_p (cm^2/Vs)	μ_n (cm^2/Vs)	$b = \mu_n/\mu_p$	THz emission (%)
InAs	0.35	0.73	500	40000	80	100
InP	1.34	0.49	200	5400	17	8.2
GaAs	1.42	0.29	400	8500	21	4.9
GaSb	0.73	0.08	1000	3000	3	0.8
InSb	0.17	0.51	850	77000	91	0.7
InN	0.68 [20]	≈2.8 [14]	39 [21]	3500 [22]	90	

Energy gap E_g, energy distance to next satellite valleys ΔE, hole- and electron mobility μ_p, μ_n.

L- and the Γ-point for the cubic III–V semiconductors. For hexagonal InN, the difference of the next satellite minimum to the Γ-point was taken. It shows that intervalley scattering is negligible for wide band gap semiconductors (InP, GaAs). However, here the absorption is too small (see Fig. 5) to generate a remarkable Dember field and, hence, the surface field will dominate the THz emission. On the other hand, InN combines a small band gap with a high mobility quotient b and a high absorption coefficient with a very high energetic distance to the satellite valleys ($\approx$2.8 eV), which cannot be populated by the applied photon energies. Recently, Polyakov et al. [28] have calculated the band structure effects on the THz emission from unbiased InN and InAs surfaces. They have shown that the energy distances between central and satellite valleys are crucial parameters for efficient THz generation and, hence, their results also underline InN as a promising THz emitter.

Finally, the Dember field is also reduced for high n-type background concentrations n_b. This dependence emphasizes the need to improve the electrical properties of InN layers, i.e. reduce n_b and increase μ_n.

5. Conclusion

In conclusion we have observed strong THz emission from different InN layers, which was shown in direct comparison to a p-InAs reference emitter. This could be explained using an extension of the theoretical models (intrinsic surface field and the photo-Dember effect) by taking into account the pecularities of the InN band structure. According to this an efficient THz surface emitter should generate a strong Dember field by: (i) a high absorption coefficient at the excitation wavelength ($\approx 10^4\,\mathrm{cm}^{-1}$), (ii) a high ratio μ_n/μ_p and (iii) a high energetic level of the satellite valleys in the band structure compared to the Γ-point in order to avoid the generation of electrons with high effective mass. In addition, the importance to control the growth processes for atomically smooth surfaces, low electron concentration and high electron mobility of InN was pointed out.

Acknowledgements

This work was supported by the FhG internal program under grant MAVO 813907, by the Thuringian ministry of culture (TKM) and the European Union (B509-04011, EFRE: B 678-03001, 6th framework: GaNano NMP4-CT2003-505614).

References

[1] B. Hu, M. Nuss, Opt. Lett. 20 (1995) 1716.
[2] A. Dobroiu, M. Yamashita, Y. Oshima, Y. Morita, C. Otani, K. Kawase, Appl. Opt. 43 (2004) 5637.
[3] H. Harde, N. Katzenellenbogen, D. Grischkowsky, J. Opt. Soc. Am. B 11 (1994) 1018.
[4] K. Kawase, Y. Ogawa, Y. Watanabe, H. Inoue, Opt. Exp. 11 (2003) 2549.
[5] M. Herrmann, M. Tani, M. Watanabe, K. Sakai, IEEE Proc-Optoelectron. 149 (2002) 116.
[6] X.-C. Zhang, B. Hu, J. Darrow, D. Auston, Appl. Phys. Lett. 56 (1990) 1011.
[7] R. Ascázubi, I. Wolke, K. Denniston, H. Lu, W. Schaff, Appl. Phys. Lett. 84 (2004) 4810.
[8] J. Wu, W. Walukiewicz, E. Haller, H. Lu, W. Schaff, Y. Saito, Y. Nanishi, Appl. Phys. Lett. 80 (2002) 3967.
[9] G. Matthäus, T. Schreiber, J. Limpert, S. Nolte, G. Torosyan, R. Beigang, S. Riehemann, G. Notni, A. Tünnermann, Opt. Commun. 84 (2005) 114.
[10] G. Chern, E. Readinger, H. Shen, M. Wraback, Appl. Phys. Lett. 89 (2006) 141115.
[11] J. Limpert, F. Röser, T. Schreiber, A. Tünnermann, IEEE JSTQE 12 (2) (2006) 233.
[12] V. Davydov, A. Klochikhin, R. Seisyan, V. Emtsev, S. Ivanov, F. Bechstedt, J. Furthmüller, H. Harima, A. Mudryi, J. Aderhold, O. Semchinova, J. Graul, Phys. State Solid (b) 229 (2002) R1.
[13] S. O'Leary, B. Foutz, M. Shur, L. Eastman, Appl. Phys. Lett. 87 (2005) 222103.
[14] F. Bechstedt, J. Furthmüller, M. Ferhat, L. Teles, L. Scolfaro, J. Leite, V. Davydov, O. Ambacher, R. Goldhahn, Phys. State Solid (a) 195 (2003) 628.
[15] K. Sakai, Terahertz Optoelectronics, Springer, Berlin, Heidelberg, 2005.
[16] V. Lebedev, V. Cimalla, J. Petzold, M. Himmerlich, S. Krischok, J.A. Schaefer, O. Ambacher, F. Morales, J. Lozano, D. González, J. Appl. Phys. 100 (2006) 094902.
[17] J. Limpert, T. Schreiber, T. Clausnitzer, K. Zöllner, H. Fuchs, E. Kley, H. Zellmer, A. Tünnermann, Opt. Exp. 10 (2002) 628.
[18] Ioffe Physico-Technical Institute, New semiconductors materials. URL <http://www.ioffe.rssi.ru/SVA/NSM/Semicond>.
[19] C. Weiss, R. Wallenstein, R. Beigang, Appl. Phys. Lett. 77 (2000) 4160.
[20] R. Goldhahn, P. Schley, A. Winzer, G. Gobsch, V. Cimalla, O. Ambacher, M. Rakel, C. Cobet, N. Esser, H. Lu, W. Schaff, Phys. State Solid (a) 203 (2006) 42.
[21] F. Chen, A. Cartwright, H. Lu, W. Schaff, Appl. Phys. Lett. 87 (2005) 212104.
[22] B. Nag, J. Cryst. Growth 269 (2004) 35.
[23] E. PalikHandbook of Optical Constants, vol. 2, Academic Press, Boston, 1993.
[24] M. Levinshtein, S. Rumyanthsev, M. Shur, Properties of Advanced Semiconductor Materials: GaN, AlN, BN, SiC, SiGe, Wiley, New York, 2000.
[25] X.-C. Zhang, D. Auston, J. Appl. Phys. 71 (1992) 326.
[26] M. Johnston, D. Whittaker, A. Corchia, A. Davies, E. Linfield, Phys. Rev. B 65 (2002) 165301.
[27] V. Cimalla, M. Niebelschütz, G. Ecke, V. Lebedev, O. Ambacher, M. Himmerlich, S. Krischok, J. Schaefer, H. Lu, W. Schaff, Phys. State Solid (a) 203 (2006) 59.
[28] V. Polyakov, F. Schwierz, Semicond. Sci. Technol. 22 (2007) 1016.
[29] R. Ascázubi, C. Schneider, I. Wilke, R. Pino, P. Dutta, Phys. Rev. B 72 (2005) 045328.
[30] V. Gavrilenko, A. Grechov, G. Korbutjak, B. Litobtschenko, Optical Properties of Semiconductors, Naukova Dumka, Kiev, 1987.